

Effect of $MgCl_2$ on Energy Generation by Reverse Electrodialysis

Ahmet H. Avci^a, Pinkey Sarkar^a, Diego Messina^b, Enrica Fontananova^b, Gianluca Di Profio^b, Efrem Curcio^{a,b}

^a Department of Environmental and Chemical Engineering, University of Calabria DIATIC-UNICAL, Via P. Bucci CUBO 45A, 87036 Rende (CS) Italy

^b Institute on Membrane Technology, National Research Council of Italy ITM-CNR, Via P. Bucci CUBO 17C, 87036 Rende (CS) Italy
ahmethalilavci@hotmail.com

One of the membrane-based technique for harvesting salinity gradient energy is Reverse Electrodialysis (RED). Most of the studies in literature are based on utilizing river and seawater by mimicking them with NaCl solutions. However, real solutions contain many different ions; this study deals with the impact of Mg^{2+} ion on power density (P_d). Investigations have been carried out using six solutions of NaCl and $MgCl_2$ prepared in varying compositions from 0 % to 100 %. Increasing Mg^{2+} concentration resulted in a remarkable decrease of P_d and open circuit voltage (OCV), and in a significant increase in stack resistance R_{stack} . Electrochemical impedance test (EIS) and ion chromatography analysis helped to clarify reasons for loss of power. In particular, it was found out that dominant negative contribution is due to increasing Cation Exchange Membrane (CEM) resistance in the presence of Mg^{2+} .

1. Introduction

According to US Energy Information Administration, world net electricity generation is expected to increase from 20 trillion to 40 trillion kWh in the coming 30 years. Coal, natural gas, nuclear and renewable energies are sources which presently satisfy the increasing demand of energy. Among all these sources, renewable energy is the fastest-growing source of electric power with an annual 2.8 % increase (U.S. Energy Information Administration, 2013). An emerging renewable energy source is Salinity Gradient Power (SGP), originally proposed for sea and river water more than 60 years ago (Pattle, 1954). The total technical potential of SGP is estimated to be around 647 gigawatts, which is 23 % of global electricity consumption. There are two common technologies which harvest SGP by utilizing membrane based processes: Reverse Electrodialysis (RED) – object of the present investigation - and Pressure Retarded Osmosis (PRO). RED is distinguished from PRO in the case of utilizing high concentration solutions like brine and seawater, instead of utilizing seawater and river water (Post et al. 2007). Possible application areas of SGP techniques are estuaries where freshwater rivers run into seawater, high salinity wastewater (brine from desalination or salt mining) and saltwater lakes (International Renewable Energy Agency, 2014). In a typical RED system, cation exchange membranes (CEM) and anion exchange membranes (AEM) are stacked alternately; driven by a concentration gradient between a Low Concentration Compartment (LCC) and a High Concentration Compartment (HCC), the diffusive flux of ions generates an electrochemical membrane potential recorded as a voltage across electrodes. In last 10 years, researches were focused mostly to increase efficiency and P_d of RED, as maximum result 2 W/m^2 power generated by using river and seawater (Vermaas et al., 2013). Nevertheless, since most of the results were obtained mimicking solutions only by using water and NaCl, further investigation is necessary to have more realistic outcome (Tufa et al., 2014; 2015). The objective of our study was to enlighten the reduction effect of Mg^{2+} on P_d and transport mechanism of ions.

2. Materials and methods

2.1 Experimental setup

A SGP-RE stack (Figure. 1) with an active membrane area of 0.01 m^2 ($10 \text{ cm} \times 10 \text{ cm}$) was operated in cross-flow mode and equipped with 25 cell pairs for all achieved experiments provided by REDstack B.V (The Netherlands). Stack basically has 2 inlet and 2 outlet channels for saline solutions, 2 electrolyte compartments continuously recirculated, a cathode and an anode. AEM-80045 and CEM-80050 were main constituents of one cell pair which were provided by Fujifilm Manufacturing Europe B.V (The Netherlands).

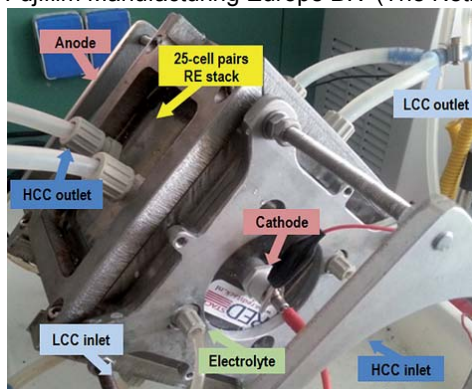


Figure 1: Salinity gradient power reverse electro dialysis unit used in experiments

Important characteristics of Ion Exchange Membranes (IEMs) are tabulated in Table. 1. Each cell pair was supported with 270 mm polyethylene gaskets and PET spacers (Deukum GMBH, Germany). Besides repeating cell units, at the both end of the stack there are electrode compartments which consist anode and cathode made of inert Ti–Ru/Ir mesh had a dimension of $10 \text{ cm} \times 10 \text{ cm}$ (MAGNETO Special Anodes B.V., The Netherlands).

Table 1: Properties of ion exchange membrane

Membrane code	Thickness (mm)	Ion exchange capacity (mmol/g membrane)	Density of fixed charge (mol/L)	Membrane area resistance (Ωcm^2)
Fuji-AEM-80045	129 ± 2	1.4 ± 0.1	3.8 ± 0.2	1.551 ± 0.001
Fuji-CEM-80050	114 ± 2	1.1 ± 0.1	2.4 ± 0.2	2.974 ± 0.001

2.2 Solutions

LCC and HCC solutions were prepared by dissolving required amount of NaCl and $\text{MgCl}_2 \cdot 6\text{H}_2\text{O}$ (Sigma-Aldrich, Italy) in deionized water (PURELAB, Elga LabWater®, $0.055 \mu\text{S cm}^{-1}$). All solutions were fed to the stack at a flow rate of 20 L/h by Masterflex L/S digital peristaltic pumps Mod. no. 7528-10 6–600 rpm (Cole-Palmer, US). The electrolyte solution was 0.3 M potassium hexacyanoferrate(II), 0.3 M potassium hexacyanoferrate(III) and 2.5 M sodium chloride (Sigma-Aldrich S.r.l., Italy). For the recirculation of electrolyte solution, Masterflex L/S digital peristaltic pump (Cole-Palmer, US) was operated at 30 L/h.

2.3 Electrochemical measurements

Representative electric circuit for RED stack and attached measurement devices are shown in Figure. 2. A high dissipation five-decade resistance box in the range of $0.1\text{--}1000 \Omega$ (CROPICO, Bracken Hill, US) was used to load the SGP-RE system. DC voltage drop across the RED stack was measured by a $3\frac{1}{2}$ digital multimeter with accuracy of $\pm 0.5 \%$ in the range of 200 mV to 200 V (Valleman, DVM760), and the current flowing across the load resistors was measured by Agilent 34422A $6\frac{1}{2}$ digit multimeter.

All the experiments were performed by varying external resistance load whereas electric potential drop (V) and current (I) were measured simultaneously by ammeter and voltmeter, respectively. After fitting a straight line for the collected data $V(V)$ vs. $I(A)$, open circuit voltage OCV (V) which is maximum obtainable voltage value, and R_{stack} (Ω) which is total resistance of stack, were calculated from Eq(1):

$$V(I) = \text{OCV} - R_{\text{stack}} I \quad (1)$$

Intercept of fitted first order linear line gives OCV value where $I = 0$ and slope of the line gives R_{stack} similarly. After having OCV and R_{stack} , P_d (W/m^2) one of the most important performance criterion of RED, can be calculated equation given by Eq(2).

$$P_d = \frac{OCV^2}{4R_{stack}} \quad (2)$$

It is also possible to obtain maximum P_d value by plotting calculated P_d vs. i (A/m^2) which follows a parabolic trendline in the form of Eq(3).

$$P_d(i) = ai^2 + bi + c \quad (3)$$

which allows to calculate maximum P_d by Eq(4).

$$P_{d,max} = c - \frac{b^2}{4a} \quad (4)$$

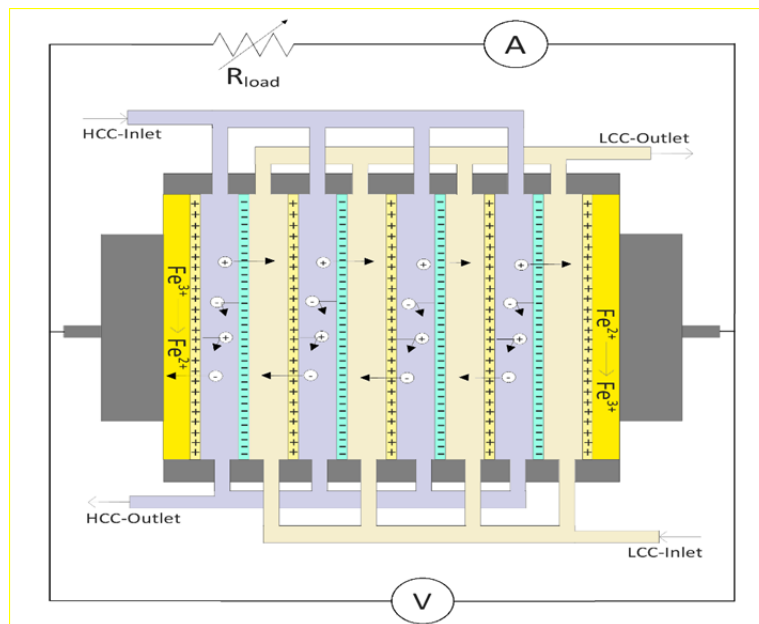


Figure 2: Electric circuit diagram of the experimental apparatus. The ammeter (A) is connected in series and voltmeter (V) connector in parallel with the resistance box (R_{load})

2.4 Impedance tests

All impedance tests were carried out by using home designed impedance test which allows 3.14 cm^2 active membrane area. Two identical solutions were fed and recirculated by using gear pumps to the cell immersed in a thermostatic bath and continuously stirred. Inside of the cell, four electrodes (working, counter, reference and sense electrodes) were arranged to apply AC current and measure potentials as shown in Figure. 3.

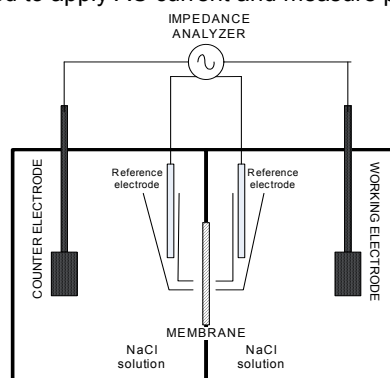


Figure 3: Schematic illustration of electrochemical impedance test

To evaluate specific resistances that contribute to total compartment resistance, a potentiostat/galvanostat combined with a frequency response analyzer, Metrohm Autolab PGSTAT302N was used. By applying AC current over a range, voltage drop through the membrane was measured. AC current in the range of 1000-0.01 Hz was generated through the cell and response was recorded in the software of Metrohm Autolab PGSTAT302N. After collecting all necessary data, an equivalent circuit model (described in section 3.2) was fitted by the help of software Nova 1.9.16 by Metrohm Autolab B.V. (Fontananova et al., 2014).

2.5 Ion Chromatography

To quantify transported ions across ion exchange membranes, Metrohm 861 Advanced Compact Ion Chromatograph was used. Characterization of anions and cations done by using Metrosep A Supp 5 - 250/4.0 and Metrosep C 4 - 250/4.0 separation column, respectively. 3.2 mM Na_2CO_3 + 1mM NaHCO_3 was used as eluent of anion column, and 2mM HNO_3 0.25mM oxalic acid was used as eluent of cation column.

3. Results

3.1 Performance of stack

Figure. 4 includes results from performance analysis of RED stack for six solutions which contain different amount of NaCl and MgCl_2 (Table 2). Best performance was achieved by using pure NaCl solution. Introduction of 10 % of MgCl_2 resulted in 20 % and 60 % decrease of OCV and P_d , respectively; a decreases of OCV and P_d up to 58 % and 94 % in the case of pure MgCl_2 solution was observed.

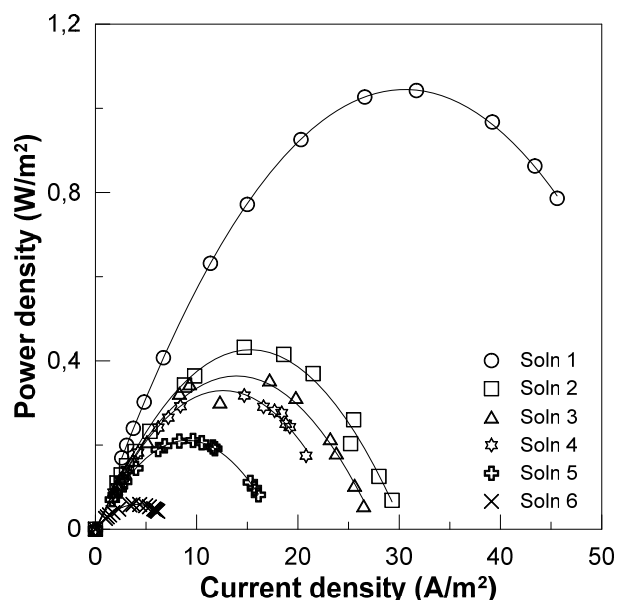


Figure 4. Gross power density vs current density

Table 2: Solutions composition, open circuit voltage (OCV), stack resistance (R_{stack}) gross power density (P_d).

Soln #	HCC Composition	LCC Composition	OCV (V)	R_{stack} (Ω)	P_d (W/m^2)
1	4.00 M NaCl	0.50 M NaCl	1.70	2.78	1.06
2	3.60 M NaCl + 0.40 M MgCl_2	0.45 M NaCl + 0.05 M MgCl_2	1.36	4.44	0.43
3	3.20 M NaCl + 0.80 M MgCl_2	0.40 M NaCl + 0.10 M MgCl_2	1.30	4.67	0.36
4	2.40 M NaCl + 1.60 M MgCl_2	0.30 M NaCl + 0.20 M MgCl_2	1.29	5.11	0.32
5	1.60 M NaCl + 2.40 M MgCl_2	0.20 M NaCl + 0.30 M MgCl_2	1.15	6.38	0.21
6	4.00 M MgCl_2	0.50 M MgCl_2	0.72	8.92	0.06

R_{stack} results refer to all components of resistance including membranes. In order to discriminate the specific contribution of a specific ion exchange membrane typology, EIS tests were carried out on CEM and AEM.

3.2 EIS tests

$$R_i = R_{m+s} + R_{dl} + R_{\Delta C} \quad (5)$$

The internal area resistance R_i (Ωm^2) of cell consists of three parts (Eq(5)): R_{m+s} arises from membrane and solution resistances, R_{dl} is related to the electrical double layer, and R_{dbl} is due to concentration polarization in the boundary layer adjacent to the membrane (Fontananova et al., 2014). The equivalent circuit model for interpretation of EIS data is shown in Figure. 5. In equivalent circuit model, 3 different resistance was taken into account in series mode. Resistance of membrane and solution represented as simple resistance, resistance of electrical double layer represented as a resistance and a capacitance in parallel and resistance of diffusion boundary layer represented as a resistance and constant phase element in parallel.

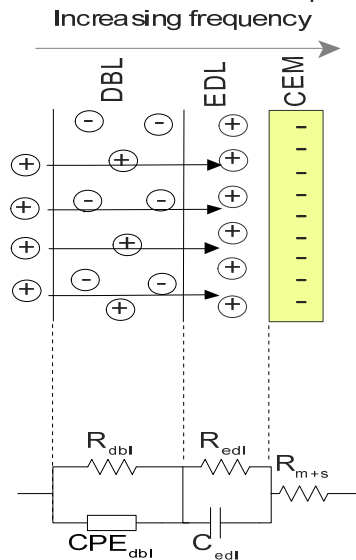


Figure 5: Resistance mechanisms on CEM and AEM (up), equivalent circuit model (down)

Table 3 reports EIS data refer to LCC solutions composition. Ohmic resistances dominate on non-ohmic ones, and R_m for CEM membranes were the most sensitive to MgCl_2 content, while R_m for AEM remained stable.

Table 3: R_m , R_{edl} , R_{dbl} , for varying MgCl_2 concentration, CEM (left) and AEM (right)

CEM				AEM			
% MgCl_2	R_m (Ωcm^2)	R_{edl} (Ωcm^2)	R_{dbl} (Ωcm^2)	% MgCl_2	R_m (Ωcm^2)	R_{edl} (Ωcm^2)	R_{dbl} (Ωcm^2)
0	2.410	0.048	0.518	0	1.350	0.014	0.131
10	6.975	0.088	0.656	10	1.493	0.008	0.069
20	9.399	0.101	0.958	20	1.369	0.009	0.061
40	15.515	0.065	1.118	40	1.269	0.008	0.059
60	18.943	0.069	1.302	60	1.459	-	-
80	20.994	-	-	80	1.370	-	-
100	23.215	0.076	0.978	100	1.407	-	-

3.3 Mass transport

Previous studies carried out by using monovalent ions show that ions' mass transfer direction is the same direction of the driving force by concentration difference; on the other hand, it is possible to find some evidence of uphill transport, i.e. mass transfer takes place in the reverse direction (Vermaas et al., 2014). In this study, in the case of cation, ion transport was observed in the same direction for monovalent Na^+ , whereas transport of Mg^{2+} is in the negative direction for solutions up to 20 % MgCl_2 content (Figure. 6).

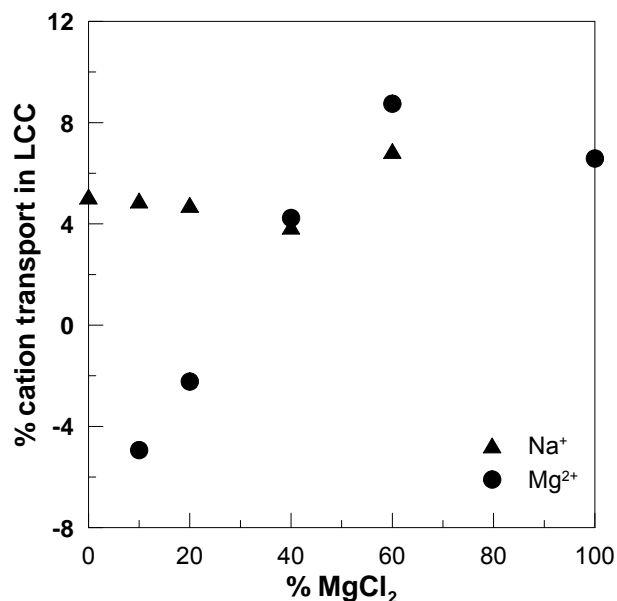


Figure 6: Percentage of immigrated ions from HCC to LCC with varying $MgCl_2$ concentration; sodium and magnesium

4. Conclusion

In this study, AEM-80045 and CEM- 80050 membranes supplied by Fujifilm were tested for energy generation by RED unit for different $NaCl/MgCl_2$ solutions. Maximum gross power density obtained was 1.06 W/m^2 when using pure $NaCl$ solutions ($LCC:HCC=0.5M:4M$), while a drastic decrease on power density was observed at increasing $MgCl_2$ content, mainly caused by the negative impact of Mg^{2+} cation on CEMs resistance. Presence of Mg^{2+} in feed solution of RED to mimic real solutions reveals that present RED membranes suffer from presence of multivalent ions. Therefore, IEM materials still need a significant improvement to compete in the field of renewable energy.

Acknowledgements

The financial support of the Education, Audiovisual and Culture Executive Agency (EU-EACEA) within the EUDIME “Erasmus Mundus Doctorate in Membrane Engineering” program (FPA 2011-0014, SGA 2014-0970, <http://eudime.unical.it>) is kindly acknowledged.

Reference

- Fontananova, E., Zhang, W., Nicotera, I., Simari, C., Baak, W.v., Di Profio, G., Curcio, E., Drioli, E., 2014, Probing membrane and interface properties in concentrated electrolyte solutions, *Journal of Membrane Science*, 459, 177-189.
- International Renewable Energy Agency (2014). Salinity Gradient Energy. Bonn, Germany.
- Pattle, R.E., 1954, Production of electric power by mixing fresh and salt water in the hydroelectric pile, *Nature*, 174, 660, DOI: 10.1038/174660a0
- Post, J.W., Hamelers, H.V.M., Buisman, C.J.N., 2009, Influence of multivalent ions on power production from mixing salt and fresh water with a reverse electro dialysis system, *Journal of Membrane Science*, 330, 65-72
- Tufa, R.A., Curcio, E., Baak, W.v., Veerman, J., Grasman, S., Fontananova, E., Di Profio, G., 2014, Potential of brackish water and brine for energy generation by salinity gradient power-reverse electro dialysis (SGP-RE), *Royal Society of Chemistry*, 4, 42617-42623
- Tufa, R.A., Curcio, E., Brauns, E., van Baak, W., Fontananova, E., Di Profio, G., 2015, Membrane Distillation and Reverse Electro dialysis for Near-Zero Liquid Discharge and low energy seawater desalination, *Journal of Membrane Science*, 496, 325-333
- Vermaas, D.A., Veerman, J., Saakes, M., Nijmeijer, K., 2014, Influence of multivalent ions on renewable energy generation in reverse electro dialysis, *Energy and Environmental Science*, 7, 1434-1445.
- U.S. Energy Information Administration (2013). International Energy Outlook 2013. Washington, US.